

Theoretical constraints on properties of low-mass neutron stars from EOS of inner crust matters

Yong-Mei Wen and De-Hua Wen*

School of Physics, South China University of Technology, Guangzhou 510641, P.R. China

(Dated: October 8, 2018)

Abstract

By employing four typical equation of states (EOSs) of the inner crust matters, the properties of low-mass neutron stars are theoretically investigated. Based on the well-known fact that there is a big gap between the neutron stars and white dwarfs in the mass-radius sequence of compact stars, according to the mass-radius relation of the four adopted EOSs, we conclude a rough forbidden-region for the central density and stellar radius to form a compact stars, that is, there is no compact star in nature having central density in the region from about 10^{12} kg/m³ to 10^{17} kg/m³, and there is also no compact star having a radius in the region from about 400 km to 2000 km. The properties of the low-mass neutron stars are also explored. It is shown that for the stable neutron star at minimum mass point, the stellar size (with radius > 200 km) is much larger than that of the normal neutron stars (with radius about 10 km), and there is a compact 'core' concentrated about 95% stellar mass in the inner core with radius within 13 km and density higher than the neutron-drip point (4.3×10^{14} kg/m³). This property is totally different from that of the normal neutron stars and white dwarfs. For a stable neutron star with stellar mass near the minimum mass, the Keplerian period is several hundred millisecond, the moment of inertia is in an order of 10^{37} kg · m², and the surface gravitational redshift is in an order of 10^{-4} .

PACS numbers: 97.20.RP;71.10.-w;04.40.Dg

* Corresponding author. wendehua@scut.edu.cn

I. INTRODUCTION

Neutron star is one of the hottest objects of study during the past decades, as neutron star provides a gold mine for the fundamental physics, including nuclear physics, astrophysics, particle physics and general relativity. Meanwhile, the nature of matter at super high densities is one of the great unsolved problems in modern science, and it is believed that neutron star is the natural and irreplaceable laboratory for investigating the super dense matters [1–4]. Therefore, among the multitudinous studies on the neutron stars, one important direction is to survey the constraints on the equation of state (EOS) of the dense matters based on the accurate and reliable observations on neutron stars, such as the fastest observed spin frequency (716Hz)[5] and the observed massive masses ($\sim 2.0M_{\odot}$) [6, 7], where both of them come from radio pulsars. In this direction, it is worth looking forward to obtaining more strict constraint on the equation of state of dense matter by measuring the radius of neutron stars to accuracies of a few percent by the next generation of hard x-ray timing instruments [3]. Another interesting direction is the theoretical researches on the EOS of the dense matter based on the experiments in terrestrial laboratory and further investigations on the structure of neutron star by using the EOS, which can provide a useful guide in primary understanding the properties of pulsars [1, 4, 8].

Presently, two characteristic parameters of the pulsars (neutron stars) have been observed very accurately, that is, the spin frequencies (or periods) and the stellar masses. More than 2400 pulsars are now observed [9]. As most of the pulsars are identified by their pulses (it is believed that the beams of radiation waves come from the magnetic pole region with one pulse per rotation. it is worth noting that in some cases, two pulses per rotation may be detected if the stars magnetic and rotation axes are nearly orthogonal [10]), this means that the spin frequencies for most of the known neutron stars have been accurately observed. Typical observed spin period is a few hundred millisecond (ms). Presently, the known spin periods of neutron stars are in a region from 1.4 ms to 12s [5, 9, 10], and based on which the neutron stars are classified as two groups: normal pulsars with spin periods $P > 30$ ms and millisecond pulsars (MSPs) with $P < 30$ ms, where MSPs comprise about 15% of the known pulsar population [9]. It is easy to understand that the massive-mass and small-size neutron star can support a very rapid spin frequency as the centrifugal force can be balanced by the super strong gravity. Theoretical investigations show that a high-mass neutron star (with mass $\sim 2M_{\odot}$) can support a sub-millisecond spin period [11, 12]; and even a low-mass neutron star still can support a relative rapid spin period (for example, a neutron star with $M \sim 0.5M_{\odot}$ can support a period ~ 2 ms) [11–13]. On the other hand, being different from the spin period observation, there are only few neutron stars having accurate stellar-mass measurements. Up to date, the number of reliable and precise mass-measured neutron stars is only 32 [14]. These samples still can not be used as an observational evidence to constrain the upper or lower mass-limit for neutron stars. Among these accurate mass-measured neutron stars, J0348+0432 has the highest mass ($M = 2.01 \pm 0.04M_{\odot}$), and J0453+1559(c) has the lowest mass ($M = 1.174 \pm 0.004M_{\odot}$)[14, 15]. In addition, the fraction of the massive NSs (with $M > 1.8M_{\odot}$) is about 20% of the observed population [14].

There is an untended inconsistency between the theoretical results and observations: the lower mass limit of the cold non-rotating neutron star is about $0.1M_{\odot}$ in theory while the observed lowest mass of neutron star is $1.174 \pm 0.004M_{\odot}$ [15, 16]. And up to date all of the observations, including the spin frequencies and the stellar masses, still can not confirm or rule out the existence of the low-mass neutron stars in the universe. Theoretically, it

is found that for the newly born proton-neutron stars, because of the larger thermal and neutrino-trapping effects, the minimum mass limit of neutron star is expected to increase to $0.9\sim 1.1 M_{\odot}$ [17, 18]. This means that a low-mass neutron star can not be produced directly by the supernova explosion. As we know, among the 2500 observed neutron stars there are only about 30 neutron stars having accurate measured-masses, and the existing knowledge still cannot rule out the possibility that there may be some low-mass neutron star in the nature. But how to form such a low-mass neutron star is still an unsolved mystery. We live in hope, there may be some unknown mechanism to form a low-mass neutron star. In fact, as an attempt, one possible mechanism has been proposed about twenty years ago [16, 19]. That is, in a binary pulsar system, if the distance between two stars is sufficiently small, the star with less mass and larger size will lose mass due to the gravitational pull by the companion star with high mass and small size. This is a self-accelerating process, because decrease of mass leads to increase of neutron star size, and vice versa. And this process makes it even more accessible for the mass loss until the less mass star reaches its minimum mass limit (M_{min}). Numerical simulations suggest that when the less mass neutron star crosses the M_{min} , it will undergo an explosion [16, 19].

One inspiring news for the neutron star observation is that the Five-hundred-meter Aperture Spherical radio Telescope (FAST), the largest single dish radio telescope in the world, has been completed by Sept. 2, 2016 in China. FAST's high instantaneous sensitivity provides the potential capacity to discover thousands of pulsars in the near future, which is far more than the number of the observed pulsars [20]. Thus, it is hopeful that FAST may increase substantially the number of the accurate-mass-measured neutron stars and even find the low-mass neutron star in the universe. On the other hand, Most of the theoretical researches focused on the normal neutron stars (with mass $\sim 1.4M_{\odot}$) or the massive neutron stars (with mass $\sim 2M_{\odot}$), but few of them concentrated on the low-mass neutron stars (with mass $< 0.5M_{\odot}$) [1, 4, 7, 8, 14]. Since there are possibilities in theory to exist the low-mass neutron stars, it is interesting to investigate them further, especially the observable quantities, which may provide useful guide for the future observation on the low-mass neutron stars. Therefore, in this work we will focus on the low-mass neutron stars, especially for those above the minimum mass limit. Moreover, if the low-mass neutron star is observed in the near future, it is also interesting to study the relations between the EOS of the inner crust and the global properties of the low-mass neutron star, as the low-mass neutron stars comprise the information of inner crust matter, in which the compositions and equation of states are not well assured yet. As we know, all the observed pulsars have fast spin frequencies. When we theoretically investigate the property of neutron star, the rotation is an important parameter. But to the cases with rotation frequency far below the Kepler frequency, where the rotation effect becomes insignificant, people often deal with the neutron stars as non-rotating stars. As a first step, here we also suppose that the low-mass neutron star considered here rotates far below its Kepler frequency, and thus can be treated as non-rotating star.

This paper is organized as follows: after a short introduction, we present the EOS of the low-mass neutron star matter in Sec. II. The structure equations and quantities of the non-rotating neutron stars are introduced in Sec. III. The detailed properties of the low-mass neutron stars and discussions are shown in Sec. IV, Conclusions and outlooks are given in the last section.

II. THE EOS OF THE LOW-MASS NEUTRON STAR MATTER

Normally, a neutron star is believed to be composed of three main parts: (1) the outer crust, with density ranging from about 10 kg/m^3 to the density of neutron-drip point $4.3 \times 10^{14} \text{ kg/m}^3$ [21]; (2) the inner crust, with density ranging from $4.3 \times 10^{14} \text{ kg/m}^3$ to the density of crust-core transition, which is about half of saturation nuclear density ρ_s , but not assured yet; (3) the uniform inner core, with density up to several times of ρ_s at the stellar center. The equation of state (EOS) of neutron star matter is a basic input for theoretical investigation on the construction of neutron star.

In the outer crust, at densities below about 10^7 kg/m^3 a fraction of electrons are bound to the nuclei; while at densities between $10^7 \text{ kg/m}^3 \sim 4.3 \times 10^{14} \text{ kg/m}^3$ the electrons are free and soon become relativistic as the density increases [21]. The EOS of the ground state of the outer crust can be well determined by using the experimental masses of neutron-rich nuclei [22]. Thus there is no distinct difference among the different models for the outer crust. In theoretical investigation on the neutron star structure, many of the researchers adopted the BPS models [4, 21] as the EOS of outer crust matter. Another improved EOS for the outer crust is established by Haensel and Pichon based on the progress in the experimental determination of masses of neutron rich nuclei [22].

The inner crust of neutron stars comprises the region from neutron-drip surface up to the crust-core transition edge, inside which the dense matter are believed to melt into the uniform liquid core. Above the neutron drip point, the energetic neutrons are no longer bound by the nuclei and the dripped neutrons form a free neutron gas. Thus, the matter in the inner crust is believed to be composed of nuclei, neutrons and electrons under the conditions of β stability and charge neutrality. The properties of nuclei in the inner crust matter are expected being very different from those of terrestrial nuclei because their properties are influenced by the gas of dripped neutrons [23]. Therefore, the EOS of the inner crust matter is still theoretical model dependent. In this work, four representative EOSs for the inner crust matter will be employed to investigate the low-mass neutron stars. They are the BBP EOS [21, 24], the NV EOS [23], the FPS21 EOS [25], and the SLY4 EOS [26]. The BBP EOS describes the nuclei by a compressible liquid-drop model to take into account the effects of the free neutrons which exert a pressure on the surface of the nuclei and thus lower the nuclear surface energy. Another important physical factor first taking into account in this model is the attractive Coulomb interaction between nuclei (that is, the lattice binding energy), which is very important in determining the size of nuclei. The NV EOS is constructed by Negele and Vautherin in 1973, which is the first group to use the Quantum calculations investigating the matter of the inner crust [23]. They determined the structure of the inner crust by minimizing the total energy per nucleon in a Wigner-Seitz sphere, and treating the electrons as a relativistic Fermi gas. The FPS21 EOS employs a generalized type of Skyrme interaction, which fits well for both the nuclear and neutron-matter calculations of Friedman and Pandharipande [25, 27]. The SLY4 EOS is based on the SLy (Skyrme Lyon) effective nucleon-nucleon interactions with a new set of improved parameters which can reproduce the new experimental data very well [26, 28]. For a detailed review for the physics of neutron star crusts, please refer to the literature [29]. The EOSs of inner crust adopted in this work are presented in Fig. 1. It is shown that the main disparity among these EOSs is in the density region from about $1.0 \times 10^{14} \text{ kg.m}^{-3}$ to $5 \times 10^{15} \text{ kg.m}^{-3}$, where FPS21 EOS, SLY4 EOS and BBP EOS are stiffer than NV EOS in the density region from about $1.0 \times 10^{14} \text{ kg.m}^{-3}$ to $8 \times 10^{14} \text{ kg.m}^{-3}$, and SLY4 EOS, BBP EOS and NV EOS are

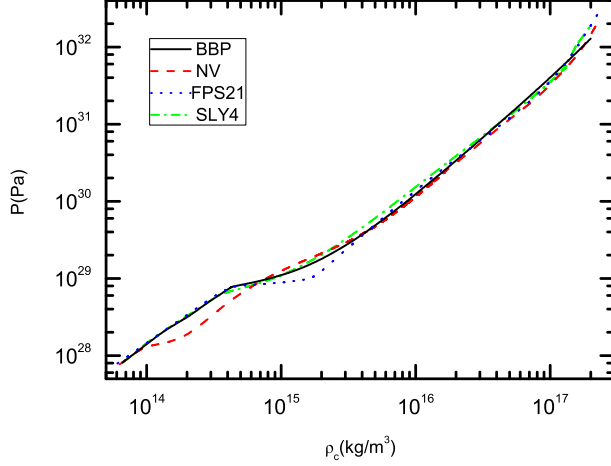


FIG. 1: The equation of states (EOSs) for the inner crust.

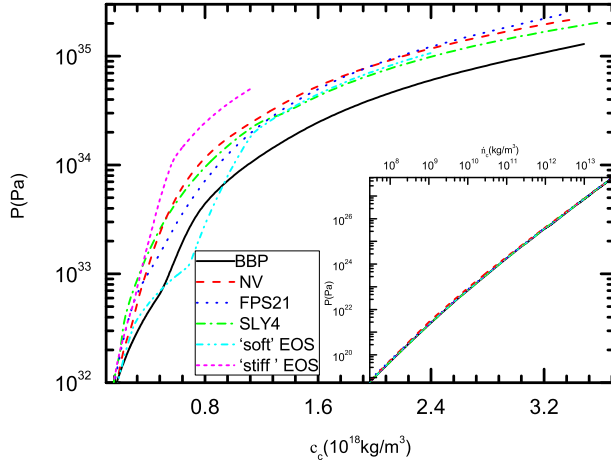


FIG. 2: The EOSs for the inner core, where the inset describes the EOSs for the outer crust.

stiffer than FPS21 EOS in the density region from about $8 \times 10^{14} \text{ kg} \cdot \text{m}^{-3}$ to $5 \times 10^{15} \text{ kg} \cdot \text{m}^{-3}$.

In order to investigate the whole sequences of the neutron stars described by different EOSs models, we also calculate the whole mass-radius relations of the compact stars from the white dwarf models up to the upper mass limit of neutron stars, where the EOSs of the inner crust are smoothly joined to the EOSs of the uniform liquid inner core and the EOSs of the outer crust based on the following literatures (For simplifying the expression of EOSs, in the following part of this paper, the EOSs combining the outer crust and the inner core are also denoted by above abbreviation of EOSs for the inner crust): (1) For the BBP EOS, the outer crust is connected by the BPS EOS, the inner core is combined by the EOS constructed by Pandharipande [30], where the parameters of the crust-core transition are $\rho_t = 2.0 \times 10^{17} \text{ kg} \cdot \text{m}^{-3}$, $n_t = 1.18 \times 10^{44} \text{ m}^{-3}$, $p_t = 1.29 \times 10^{32} \text{ pa}$ [21], and the whole data of the joined EOS are taken from Ref. [21]; (2) For the NV EOS, the

EOS of the outer crust is taken from the work of Harrison and Wheeler [31], the DBHF EOS is employed to describe the inner core [32], where the parameters of the crust-core transition are $\rho_t = 2.0 \times 10^{17} \text{kg} \cdot \text{m}^{-3}$, $n_t = 1.17 \times 10^{44} \text{m}^{-3}$, $p_t = 1.37 \times 10^{32} \text{pa}$ [23, 33], and the whole data of the joined EOS are taken from Ref. [33]; (3) For the FPS21 EOS, the EOS of the outer crust is constructed by Haensel and Pichon [22], the inner core is joined by the famous APR EOS [34], where the parameters of the crust-core transition are $\rho_t = 1.8 \times 10^{17} \text{kg} \cdot \text{m}^{-3}$, $n_t = 0.98 \times 10^{44} \text{m}^{-3}$, $p_t = 0.8 \times 10^{32} \text{pa}$ [25], and the whole data of the joined EOS are kindly provided by Mr. Krastev [12]. (4) For the SLy4 EOS, the outer crust is also connected by the model of Haensel and Pichon [22], and the inner core is described by the SLy4 model [28], where the parameters of the crust-core transition are $\rho_t = 1.28 \times 10^{17} \text{kg} \cdot \text{m}^{-3}$, $n_t = 0.76 \times 10^{44} \text{m}^{-3}$, $p_t = 0.54 \times 10^{32} \text{pa}$ [26], and the whole data of the joined EOS are taken from Ref. [26]. In fact, the transition region from the highly ordered crystal to the uniform liquid core is complicated and is poorly understood, and up to date, the transition density is still very divergent [2, 23, 24, 26, 35, 36]. Fortunately, the position of the crust-core transition edge is mainly responsible for such as the glitches, and does not directly effect the mass-radius relation and the lower mass limit for a certain EOS. By the way, people often use 'softness' or 'stiffness' to describe an EOS, where a softer EOS means that at a fixed density the pressure is relative lower, while a stiffer EOS corresponds to a higher pressure [4, 6, 37, 38]. In fact, the softness and stiffness for an EOS is relative. A clear express should include the density domain and the comparison object. For example, the NV EOS is stiffer than most of the other considered EOSs at higher density region (as shown in Fig. 2), while it is softer than other EOSs in density region $1.0 \times 10^{14} \text{kg} \cdot \text{m}^{-3} \sim 8 \times 10^{14} \text{kg} \cdot \text{m}^{-3}$ and $10^{16} \text{kg} \cdot \text{m}^{-3} \sim 10^{17} \text{kg} \cdot \text{m}^{-3}$ (as shown in Fig. 1). In this work, unless otherwise specified, when we talk about the softness (or stiffness) of an EOS, the density domain is in $10^{14} \text{kg} \cdot \text{m}^{-3} \sim 10^{17} \text{kg} \cdot \text{m}^{-3}$, that is, for the matter in inner crust; and the comparison objects are the four considered EOSs.

The EOSs for the inner core are presented in Fig. 2, where the EOSs of the outer crust is shown in the inset. It is shown that for all of the adopted EOSs, the EOSs of the outer crust matter are similar. And for the inner core, BBP EOS is relatively softer. For comparing with the new progress of EOSs, we also plot the high density part of 'soft' and 'stiff' EOSs of Ref. [38] in Fig. 2, where the crust are connected by the BBP EOS (denote as BPS in the Ref. [38]). It is shown that the 'soft' EOS is still stiffer than BBP EOS at higher density ($> 3\rho_0$). In order to express conformable with the reference and also do not make confusion in this work, here we add an apostrophe to denote these two EOSs.

III. STRUCTURE EQUATIONS OF NON-ROTATING NEUTRON STARS

Supposing that the matter of a neutron star can be treated as perfect fluid, then its energy-momentum tensor can be described as

$$T^{\alpha\beta} = pg^{\alpha\beta} + (p + \rho)u^\alpha u^\beta, \quad (3.1)$$

where $\alpha, \beta = 0, 1, 2, 3$, u^α is the four-velocity satisfying $u^\alpha u_\alpha = -1$, ρ is the density and p is the pressure. Unless otherwise noted, we use geometrical unit ($G = c = 1$). A non-rotating spherically symmetric neutron star is described by the following metric

$$-ds^2 = -e^{2\Phi} dt^2 + e^{2\Lambda} dr^2 + r^2(d\theta^2 + \sin^2\theta d\phi^2), \quad (3.2)$$

where Φ and Λ are the functions of radius r only. According to the Einstein field equation

$$R^{\alpha\beta} - \frac{1}{2}g^{\alpha\beta}R = 8\pi T^{\alpha\beta} \quad (3.3)$$

and combining it with Eqs.(2) and (3), one can obtain the non-rotating neutron star structure equations, namely, the familiar Tolman-Oppenheimer-Volkoff (TOV) equations[39, 40]

$$\frac{dp}{dr} = -\frac{(p + \rho)[m(r) + 4\pi r^3 p]}{r[r - 2m(r)]}, \quad (3.4)$$

where

$$m(r) = \int_0^r 4\pi r'^2 \rho dr'. \quad (3.5)$$

The EOS of the neutron star matter is a necessary input to solve the TOV equations. We can integrate outwards from the origin ($r = 0, \rho = \rho_c$) to the point $r = R$, where the pressure becomes zero. This point defines R as the radius of the star and $M = M(R)$ as the total mass of the star.

Except for the mass and the radius, there are several other interesting global quantities characterizing the neutron stars, such as the moment of inertia, the redshift, etc. Because of the strong gravity in neutron star, these quantities are normally calculated in general relativistic theory. For the non-rotating neutron star, its moment of inertia can be calculated by [11, 41]

$$I = \frac{8\pi}{3} \int_0^R e^{-\Phi} \frac{p + \rho}{\sqrt{1 - \frac{2m(r)}{r}}} r^4 dr, \quad (3.6)$$

where the rotational effect in the original equation is neglected. As we only pay attention to the low-mass neutron star in this work, where the compactness ($2M/R$) is very small (in an order of 10^{-2} to 10^{-3} , even reduced to 10^{-4} at the minimum mass point), far smaller than that of a normal neutron star, so it is enough to calculate the moment of inertia in Newtonian gravity, that is

$$I = \frac{8\pi}{3} \int_0^R \rho r^4 dr. \quad (3.7)$$

The surface gravitational redshift can be simply calculated by

$$Z = \left(1 - \frac{2M}{R}\right)^{-1/2} - 1 \quad (3.8)$$

For a star formed by perfect fluid, there exists a maximal rotating frequency at which there comes into being a balance of gravitational and centrifugal forces at the star's equator. Exceeding the maximal frequency, the star will engender mass shedding. This maximal frequency is named as Kepler frequency. Similarly, because of the relative weaker gravity of the low-mass neutron star, we also calculate the Kepler frequency here in the Newtonian gravity frame, that is

$$P_K = 2\pi \sqrt{\frac{R^3}{M}}. \quad (3.9)$$

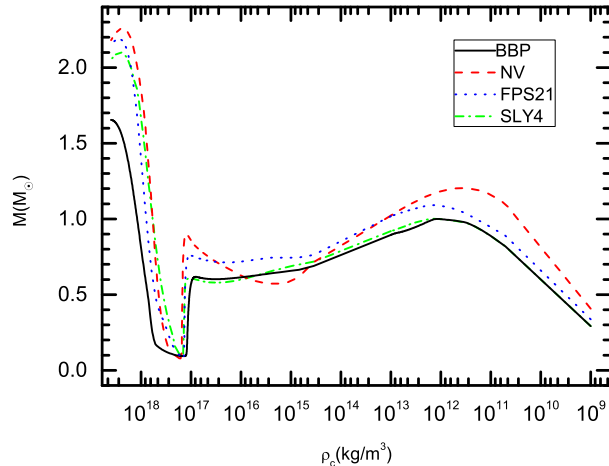


FIG. 3: The stellar masses as a function of the central densities for the four adopted EOSs, where the central density ranges from 10^9 kg/m^3 to $4 \times 10^{18} \text{ kg/m}^3$ and the star sequence covers from white dwarfs to neutron stars.

IV. THE PROPERTIES OF THE LOW-MASS NEUTRON STARS

Theoretical investigation on the minimum mass for neutron stars has a long history. The first estimate of minimum mass M_{min} , which is about $0.17 M_{\odot}$ without taking into account the nuclear interactions, was obtained by Oppenheimer & Serber [42]. Updated research shows that the minimum mass is around $0.09 M_{\odot}$ and has a weakly EOS dependence [26]. For a low-mass neutron star in binary system, if it loses its mass below the minimum mass M_{min} through gravitational pull by the companion star, an explosion will be undergone [16, 19]. On the other hand, for the stars sequence in the $M - \rho_c$ curve with central densities ρ_c smaller than that of M_{min} , where $dM/d\rho_c < 0$, as shown in Fig. 3, equilibrium configuration will also do not exist, as it will become unstable with respect to small radial perturbations [43, 44]. Thus, we only need to care for the stable low-mass neutron stars with mass above the minimum mass M_{min} .

In order to find the common characters and also show the effect of the EOSs on the low-mass neutron stars, we choose four typical EOSs of the inner crust, as have been described in Sec. II, to investigate the properties and structures of the low-mass neutron stars. For convenient to understand the whole star sequence and where the low-mass neutron stars located, we plot the $M - \rho_c$ relations in Fig. 3 and $M - R$ relations in Fig. 4 in a wide central density region (from 10^9 kg/m^3 to $4 \times 10^{18} \text{ kg/m}^3$). And in order to compare our results with that of the new progress of EOS, the $M - R$ relations of the 'soft' and 'stiff' EOSs of Ref. [38] are also plotted in Fig. 4. It is shown that there is no distinct difference between the 'new' EOSs and the 'old' EOS at the low-mass region for stable neutron stars.

As we know, white dwarfs are the lowest density sequence of stable compact stars, where the central densities take a range from about 10^9 kg/m^3 to 10^{12} kg/m^3 , as shown in Fig. 3. From a microscopic point of view, in a stable white dwarfs the inward gravity is balanced by the pressure of degenerate electrons. As the mass of white dwarf increases, the central density and thus the Fermi energy of electrons also rise. When the Fermi energy of electron reaches a point at which the energetical electrons can be captured by protons through inverse

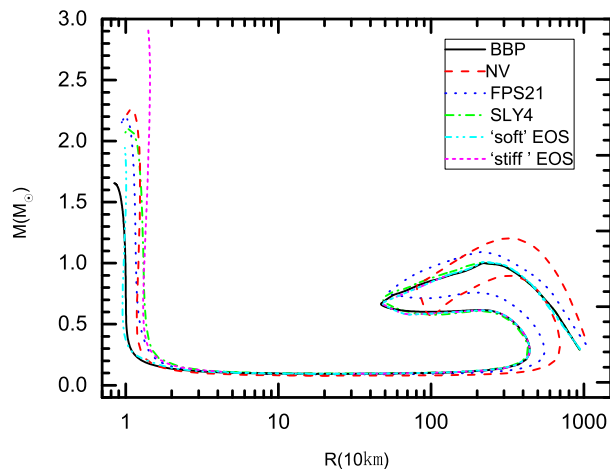


FIG. 4: The mass-radius relations for the four adopted EOSs. For comparison, the mass-radius relations for the 'soft' and 'stiff' EOSs of Ref. [38] are also plotted.

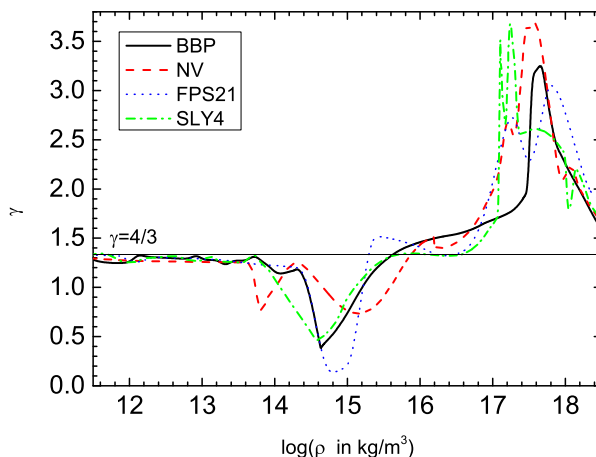


FIG. 5: The adiabatic indices in the density ranging from $3 \times 10^{11} \text{ kg/m}^3$ to $3 \times 10^{18} \text{ kg/m}^3$ as a function of the density for the four adopted EOSs.

beta decay, the pressure of the relativistic electrons stops increasing along with the density increasing, while the neutrons produced by the inverse beta decay are still bound in the neutron-rich nuclei until the neutron-drip point ($4.3 \times 10^{14} \text{ kg/m}^3$) reaches. Thus there is not enough pressure to support the strong gravity when the central density of a star becomes higher than that of the white dwarf with Chandrasekhar mass limit ($1.44M_{\odot}$) until the pressure of degenerate neutrons becomes stronger enough to balance the gravity [44]. From a macroscopic point of view, if the EOS of a star can be approximated by

$$p = K\rho^{\gamma} \quad (4.1)$$

with K a constant coefficient and γ the adiabatic index, then the mass and radius have the

relationship [44]

$$R \sim M^{(\gamma-2)/(3\gamma-4)}. \quad (4.2)$$

In order to satisfy the necessary stable condition [44]

$$\frac{\partial M(\rho_c)}{\partial \rho_c} > 0, \quad (4.3)$$

one must have

$$\gamma > 4/3. \quad (4.4)$$

While for the ultra-relativistic electron (with density $\rho \gg \rho_c \sim 10^9 \mu \text{ kg} \cdot \text{m}^{-3}$, where μ is the number of nucleons per electron [45]), its polytropic index $\gamma = 4/3$. This polytropic index sets the famous Chandrasekhar mass limit for white dwarfs. Beyond the density about $10^{12} \text{ kg} \cdot \text{m}^{-3}$ neutronization will destabilize the white dwarfs, until the pressure of degenerate neutrons dominates the balance against inward gravity. As an approximative and qualitative discussion for the star's stability, we suppose that the tabulated EOSs also can be approximatively expressed by $p = K\rho^\gamma$ and the adiabatic index can be calculated through $\gamma = \frac{d \ln(p)}{d \ln(\rho)}$. In Fig. 5, we plot the adiabatic indices of the four adopted EOSs in the density ranging from $5 \times 10^{11} \text{ kg} \cdot \text{m}^{-3}$ to $10^{17} \text{ kg} \cdot \text{m}^{-3}$. It is shown that in the density ranging from $\sim 10^{12} \text{ kg} \cdot \text{m}^{-3}$ to $\sim 10^{15} \text{ kg} \cdot \text{m}^{-3}$, the adiabatic indices of the four EOSs are less than $4/3$. Obviously, a central density in this density region cannot support a stable star. As to the stars with central densities ranging from $\sim 10^{15} \text{ kg} \cdot \text{m}^{-3}$ to $\sim 10^{17} \text{ kg} \cdot \text{m}^{-3}$, though the adiabatic indices in this density region start to become larger than $4/3$, the star sequences of the EOSs still cannot obey the necessary stable condition $\frac{\partial M(\rho_c)}{\partial \rho_c} > 0$, as shown in Fig. 3. That is, in this density region the stars are still unstable (We guess that one possible reason for this case may be that we cannot approximate the tabulated EOSs by a single polytropic form in such a wide density region). Because of the reason discussed above, we conclude that between the white dwarfs and neutron stars there exists a wide forbidden region for the central densities (from about $10^{12} \text{ kg} \cdot \text{m}^{-3}$ to $10^{17} \text{ kg} \cdot \text{m}^{-3}$) to form a compact star, as shown in Fig. 3. Correspondingly, for the same reason, we can conclude a rough size forbidden-region for the compact stars according to the four adopted EOSs in this work, that is, there is no compact star having a radius in the region from about 400 km to 2000 km, as shown in Fig. 4. It is also shown in this figure that in the stable neutron star sequence, when the stellar mass smaller than about $0.2 M_\odot$, the radius will increase rapidly as the stellar mass decreases. Before the stellar mass reaches the M_{min} , the radius of neutron star can increase over 200 km, which is far larger than the size of the normal neutron stars, this point can be seen more clearly in Fig. 6. The larger size is the main characteristics of the neutron star with mass around the M_{min} .

Based on the TOV equations, one EOS of dense matter determines a unique sequence of mass-radius of neutron stars. That is, the solutions provide a unique map between the pressure-density relation $P(\rho)$ and the mass-radius $M(R)$ relation of stars [46]. This unique mapping provides a useful way to infer the EOS of dense matter from astrophysical observations of a set of neutron stars with both mass and radius observed-values. The measurement of the low-mass neutron stars in the future is a key factor for the entire mass-radius relation if we want to constrain the EOS very well by this way. As it has been mentioned in Sec. II,

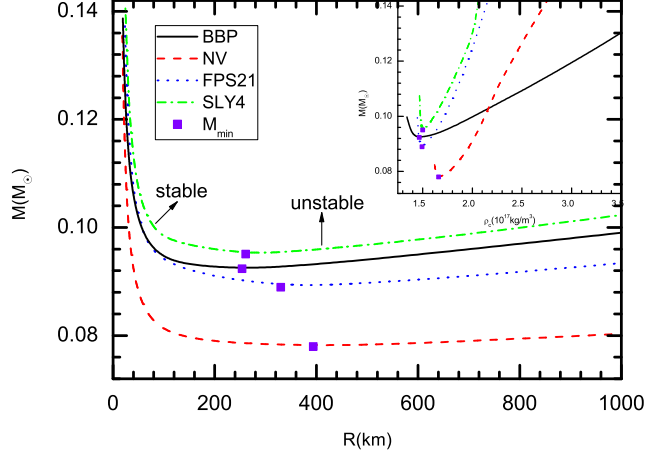


FIG. 6: The mass-radius relations for the low-mass neutron stars, where the inset is the masses as a function of the central densities, and the small square on the line denotes the M_{min} point.

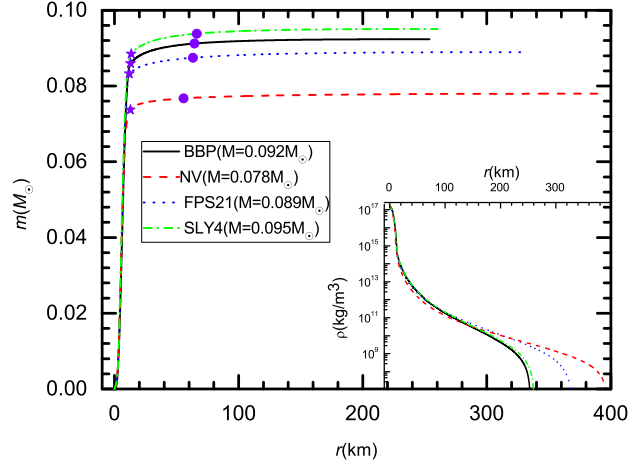


FIG. 7: The mass profile for the neutron star with minimum mass, where the stars mark the points with density at neutron-drip point and the circles mark the points at density 10^{12} kg/m^3 . The inset is the corresponding density profile.

TABLE I: the properties of non-rotating neutron stars at minimum mass points

EOS	M/M_{\odot}	R (km)	ρ_c (10^{17} kg/m^3)	P (s)	I ($10^{37} \text{ kg} * \text{m}^2$)	Z (10^{-4})
BBP	0.092	254	1.466	0.230	2.53	5.37
NV	0.078	394	1.660	0.483	3.39	2.92
FPS21	0.089	330	1.493	0.346	3.56	3.98
SLY4	0.095	261	1.501	0.236	2.80	5.38

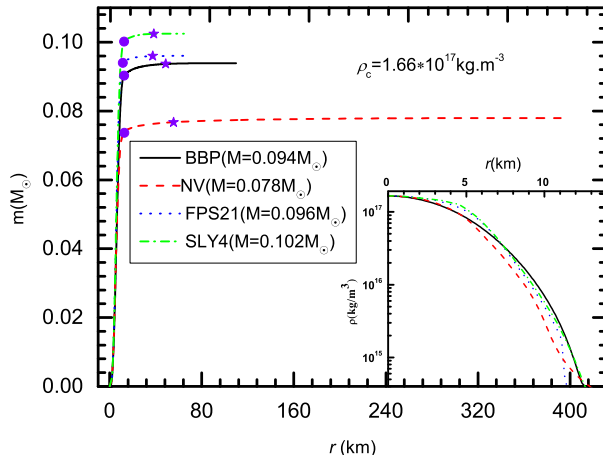


FIG. 8: The mass profile for the neutron star at central density $1.66 \times 10^{17} \text{ kg/m}^3$, where the stars mark the points with density at neutron-drip point and the circles mark the points at density 10^{12} kg/m^3 . The inset is the density profile for the inner core with density $> 4 \times 10^{14} \text{ kg/m}^3$.

TABLE II: the properties of non-rotating neutron stars at the crust-core transition density ρ_t (For SLY4 EOS, the star with $\rho_c = \rho_t$ is unstable)

EOS	M/M_\odot	R (km)	ρ_c (10^{17} kg/m^3)	P (ms)	I ($10^{36} \text{ kg} * \text{m}^2$)	Z (10^{-3})
BBP	0.100	56.2	2.0	23.0	5.10	2.60
NV	0.091	42.4	2.0	15.8	3.49	3.10
FPS21	0.106	40.7	1.8	13.8	4.67	3.91

the EOS of the inner crust matter is very difficult to be determined by the terrestrial experiments because of the gas of dripped neutrons, thus the astrophysical measurements for the low-mass neutron stars become very important to accurately determine the EOS of the dense matter, including that of the inner crust. It has been turned out that EOSs have certain characteristics that make it possible to qualitatively infer the stellar properties from some special density region. For the normal neutron stars, it is found that the maximum mass is determined primarily by the behavior of EOS at the highest densities (about $7 \sim 8\rho_0$, where ρ_0 is the saturation density) and the slope of the mass-radius relation depends mostly on the pressure at $\sim 4\rho_0$ [47]; while the radius depends primarily on the pressure at $\sim 2\rho_0$ [48]. Encouraged by these interesting works, as a first step, we will primarily investigate the properties of the low-mass neutron stars, which may be helpful for us in theoretically understanding the map between $P(\rho)$ and $M(R)$ at the low-mass part for neutron stars.

The property values of neutron stars at M_{min} points are presented in Tab. I. It is shown that three of the EOSs (BBS, FPS21, SLY4) give a M_{min} around $0.09 M_\odot$, while NV EOS gives a relatively smaller minimum mass with $M_{min} = 0.078 M_\odot$. The difference between the NV EOS and other three EOSs may provide a clue to understand the effect of softness of crust EOS on the properties of the low-mass neutron stars. As the central densities of the neutron stars at M_{min} points are below the saturation density of nuclear matter (as shown in Tab. I), so the properties of the stars at M_{min} points are only sensitive to the EOSs at

subnuclear densities. In order to show the properties of the low-mass stable neutron stars around minimum mass point more clearly, the $M - R$ relations and $M - \rho_c$ relations (the inset) around the M_{min} points are plotted in Fig. 6. It is shown that among the four adopted EOSs, the NV EOS, which is relative softer in the density region $10^{14} \text{ kg.m}^{-3} \sim 10^{15} \text{ kg.m}^{-3}$ and $10^{16} \text{ kg.m}^{-3} \sim 10^{17} \text{ kg.m}^{-3}$, has a higher central density, a smaller M_{min} and a larger radius at the M_{min} point.

For analyzing the properties of the neutron star around the M_{min} points, we plot the mass profiles of neutron stars at M_{min} points in Fig. 7, where the stars mark the points with density at neutron-drip point and the circles mark the points at density 10^{12} kg/m^3 , and the inset is the density profile. It is shown that for the stable neutron star at minimum mass point, there is a compact 'core' concentrated about 95% stellar mass in the inner core with radius within 13 km and density higher than the neutron-drip point ($4.3 \times 10^{14} \text{ kg/m}^3$). Another representative density point (10^{12} kg/m^3) is also marked in Fig. 7, where the mean radius r is about 60 km and the mass $m(r)$ is about 99% of $M(R)$. These results show that for the minimum-mass stable neutron star, most of the stellar mass is composed of the crystal lattice of neutron-proton clusters immersed in electron gas and is located in a small space in the center, while most of the stellar space is filled of low dense matter. These properties are totally different from the normal neutron stars, where there is only a very thin outer crust ($\rho < 4.3 \times 10^{14}$). In fact, for both of the normal neutron stars and white dwarfs, there is no such a compact 'core' like the minimum-mass stable neutron star, as shown in Fig. 3.11 and Fig. 3.12 in Ref. [44].

Why a softer EOS will give a lower M_{min} ? In what follows we will give a qualitative discussion. For low-mass neutron star, it is reasonable to ignore the general relativistic effect. Thus the TOV pressure equation can be approximated as

$$\frac{dp}{dr} = \frac{\rho m(r)}{r^2}, \quad (4.5)$$

which is just the hydrostatic equilibrium equation in Newtonian gravity. Near the central, fixed r and dr (for example, $r=10\text{m}$, $dr=1\text{m}$), a higher central density will give a higher ρ and thus a larger $m(r)$ ($\approx 4/3\pi r^3 \rho$), which leads to a larger dp . For a softer EOS (e.g. NV EOS), a larger dp corresponds with a larger $d\rho$, which leads to a faster density decrease. For example, at $r=10 \text{ km}$, $\rho_{BBP}=8.2 \times 10^{15} \text{ kg.m}^{-3}$, $\rho_{NV}=3.5 \times 10^{15} \text{ kg.m}^{-3}$, $\rho_{FPS21}=6.1 \times 10^{15} \text{ kg.m}^{-3}$, $\rho_{SLY4}=6.8 \times 10^{15} \text{ kg.m}^{-3}$. It is clear that the softer NV EOS has a faster density decrease. In fact, in the inner 10 km, the mass $m(r)$ occupies about 90% of the the total stellar mass. So it is easy to understand that why a softer EOS for the inner crust gives a smaller M_{min} . In order to address this point in another way, we plot the mass profile and the density profile (the inset, only with density $> 4 \times 10^{14} \text{ kg/m}^3$) at a fixed central density ($1.66 \times 10^{17} \text{ kg/m}^3$, which is the central density of NV EOS at its minimum-mass point) in Fig. 8. It is shown that at the same central density, the softer NV EOS gives a lower stellar mass. In the inset, it is clear shown that the softer NV EOS has a faster density decrease in the inner core.

There is another interesting phenomenon that the density profiles (see the inset in Fig. 7) show distinct difference at density lower than $10^{11} \text{ kg.m}^{-3}$ while the EOSs at this density region are nearly the same (see the inset in Fig. 2). In fact, this difference does not come from the difference of the low density region, but comes from the mass $m(r)$ distribution inner the star with radius of r . As 99% of stellar mass is distributed in the inner part where density is higher than $10^{11} \text{ kg.m}^{-3}$, so we can replace $m(r)$ by the total stellar mass $M(R)$ in

discussing the structure of the low density part. For the star's outer part with lower density ($< 10^{11} \text{ kg}\cdot\text{m}^{-3}$), ignoring the general relativistic effect, Eq. 4.5 can be approximated as

$$\frac{dp}{dr} = \frac{\rho M(R)}{r^2}. \quad (4.6)$$

As the EOSs in this density region are similar, it is easy to understand that with a fixed dp , a smaller stellar mass $M(R)$ will give a larger dr , and finally lead to a relatively larger stellar radius. We can also qualitatively understand this in another way. For a neutron star based on NV EOS, as it has a core with lower mass, the gravitational potential at its outer crust is thus weaker than that of a neutron star based on the other EOSs in Fig.8, which leads to a relative incompact matter distribution and therefore result in a larger stellar radius.

Beside the mass-radius relation, it is expected there are other observable properties for the low-mass neutron stars can also provide constraints on the EOSs of the inner crust matter. As a first step, we will investigate three properties of the low-mass neutron stars based on the currently available EOSs for the inner crust matter, which may be helpful in extracting the constraint on the EOSs of the crust matter in the future observations on the low-mass neutron stars. These three properties are the spin period at Keplerian frequency, the moment of inertia and the redshift, which are presented in Figs. 9-11, respectively. Meanwhile, in order to quantitatively show them, we also present the property parameters at M_{min} points and at crust-core transition densities in Tabs. I and II, respectively. It is shown that for a neutron star at minimum mass M_{min} , its Keplerian period is several hundred millisecond, which is beyond the period of a millisecond pulsars, but still in the region of the observed pulsars periods. From this point of view, we can not rule out the possibility that some of the observed pulsars may have very lower stellar mass. As shown in Fig.9, around the M_{min} point, as the central density increases, the Keplerian period decreases very quickly. When the stellar mass increases up to about $0.1 M_{\odot}$, as shown in Tabs. II, the star can finish a spin in about 20 ms, which already lies in the period region of millisecond pulsars. Moreover, because of the larger size, we can qualitatively expect that a low-mass neutron star around the M_{min} point may have a notable rotation deformation under the rapid spin.

It has been recognized that the measurement of spin-orbit coupling provides a way to determine the moment of inertia of a star in a double pulsar system [49, 50]. As the moment of inertia of a star is close related to its mass and radius, if the mass and the moment of inertia are observed for the same neutron star, the radius can be determined very well, and then the EOS can be constrained strictly. As a first step, the theoretical expected value of the moment of inertia for the low-mass neutrons star is studied here. Near the minimum mass point, because of the larger size (with radius about 200 km), the moment of inertia is in an order of $10^{37} \text{ kg} \cdot \text{m}^2$, as shown in Tab. I and Fig. 10. Near the minimum mass point, due to the rapid decrease of radius as the central density increasing, the moment of inertia decreases very quickly. At a stellar mass about $0.1 M_{\odot}$, the moment of inertia is in an order of $10^{36} \text{ kg} \cdot \text{m}^2$, as shown in Tab. II. By the way, for a normal neutron star with mass of $1.4 M_{\odot}$, its moment of inertia is in an order of $10^{38} \text{ kg} \cdot \text{m}^2$ [11, 51].

The measurement of redshift provides another way to constrain the radius and EOS of compact stars [52]. For a low-mass neutron star near the minimum mass point, because of the smaller mass and the larger size, the surface gravitational redshift is very tiny, with an order of 10^{-4} , as shown in Tab. I, which is approximately three orders of magnitude less than that of the normal neutron star [11, 52]. This result reminds us that if a very tiny redshift is observed related to a pulsar in the future, it is a clue that there is a low-mass neutrons

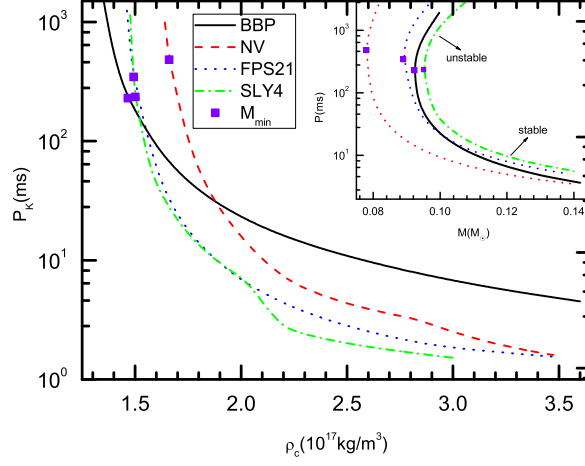


FIG. 9: The Keplerian period (P_K) as a function of the central density ρ_c , where P_K denotes the period of a star rotating at Keplerian frequency. The inset shows the $P_K - M$ relations.

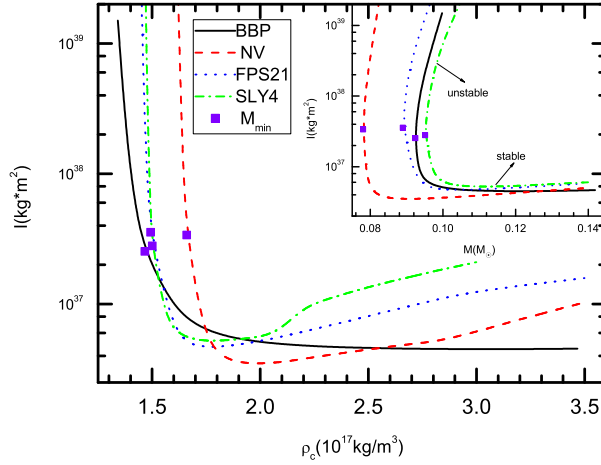


FIG. 10: The moment of inertia I as a function of the central density ρ_c . The inset shows the $I - M$ relations.

star. It is also because of the rapid decrease of radius as the central density increasing, the redshift has a two orders of magnitude increase in the mass region from the minimum mass point to about $0.2 M_\odot$, as shown in the inset of Fig. 11.

In the end, we present a brief discussion for the rotation effect on the minimum mass and radius of neutron star. Theoretically, at a fixed central density, a lower mass neutron star has a slighter rotation effect on both the stellar mass and radius at its Kepler frequency, as the lower mass neutron star only can support a slower Kepler frequency, and thus only causes a smaller centrifugal force [11, 13]. The fastest observed spin frequency of pulsar is 716 Hz (corresponding with a period of 1.4 ms) [5]. For the FPS21 EOS, in order to support such a spin frequency, its stellar mass must be larger than about $0.8 M_\odot$ (See Fig. 7 in Ref. [11], where the FPS21 EOS is denoted as APR). Therefore, it is easy to understand

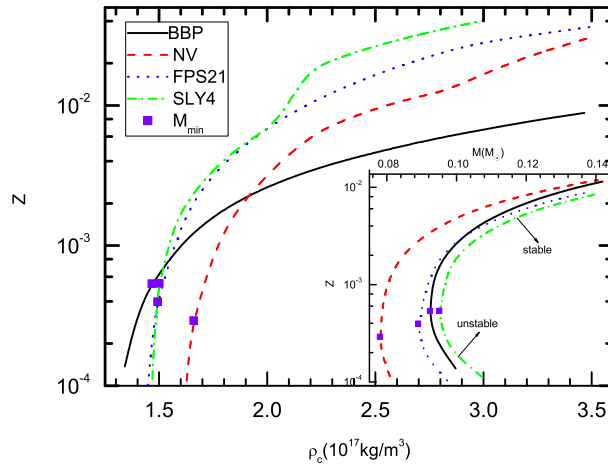


FIG. 11: The redshift z as a function of the central density ρ_c . The inset shows the $z - M$ relations.

that when the rotation effect is taken account of, the minimum mass of stable neutron star supported by an EOS is determined by the fast spin frequency (no longer the lowest point in the mass-radius sequence). For the detailed discussion for the rotation effect on the minimal mass and radius of neutron star, please refer to Ref. [16].

V. CONCLUSIONS

Up to date, all of the observations still can not confirm or rule out the existence of the low-mass neutron stars in the universe. Moreover, we also cannot rule out the existence of the low-mass neutron stars in theory. As most of the theoretical researches focused on the normal neutron stars (with mass $\sim 1.4M_\odot$) or the massive neutron stars (with mass $\sim 2M_\odot$) and few of them concentrated on the low-mass neutron stars (with mass $< 0.5M_\odot$), and also because that there is a close relation between the low-mass neutron star and the EOS of the inner crust matter, thus it is interesting to carry out an investigation on the low-mass neutron stars. In this paper, by employing four typical equation of states (EOSs) for the inner crust, we investigate the detailed properties of the low-mass neutron stars. Based on the well-known fact that there is a big gap between the neutron stars and white dwarfs in the mass-radius sequence of compact stars, according to the mass-radius relation of the four adopted EOSs, we conclude a rough forbidden-region for the central density and stellar radius to form a compact stars, that is, there is no compact star in nature having central density in the region from about 10^{12} kg/m^3 to 10^{17} kg/m^3 , and there is also no compact star having a radius in the region from about 400 km to 2000 km. Limited by the EOS samples, we only conclude here a rough forbidden-region for the compact stars. If more precise EOS or more EOS samples for the crust matter are obtained in the future, one can give a stricter forbidden-region. The properties of the low-mass neutron stars are analyzed. It is shown that for the stable neutron star at minimum mass point, the stellar size (with radius > 200 km) is much larger than that of the normal neutron stars (with radius about 10 km), and there is a compact 'core' concentrated about 95% stellar mass in the inner core with radius within 13 km and density higher than the neutron-drip point ($4.3 \times 10^{14} \text{ kg/m}^3$).

This property is totally different from that of the normal neutron stars and white dwarfs.

Three quantities of the low-mass neutron stars (the spin period at Keplerian frequency, the moment of inertia and the redshift), are calculated and discussed. It is found that for a stable neutron star with stellar mass near the minimum mass, the Keplerian period is several hundred millisecond, which is beyond the period of a millisecond pulsars, but still in the region of the observed pulsars periods; the moment of inertia is in an order of $10^{37} kg \cdot m^2$; and the surface gravitational redshift is in an order of 10^{-4} .

If the new observation apparatuses find the low-mass neutron star in the future, it will provide a way to constrain the EOSs of nuclear matter at subnuclear densities strictly. Thus it will be an interesting topic to investigate the inverse stellar structure problem to determine the equation of state of the matter at subnuclear densities.

Acknowledgments

We would like to thank G. C. Yong and X. D. Zhang for helpful discussion and the referee for helpful comments and suggestions. This work is supported by NSFC (Nos. 11275073 and 11305063). This project has made use of NASA's Astrophysics Data System.

-
- [1] J.M. Lattimer, M. Prakash, *Science* **304**, 536(2004).
 - [2] J. Piekarewicz, *AIP Conf. Proc* **1595**, 76(2014).
 - [3] A.L. Watts, N. Andersson, D. Chakrabarty, M. Feroci, *Rev.Mod.Phys* **88**, 021001 (2016).
 - [4] J.M. Lattimer, M. Prakash, *Phys. Rep* **621**, 127(2016).
 - [5] J.W.T. Hessels, S.M. Ransom, I.H. Stairs, P.C.C. Freire, V.M. Kaspi, F. Camilo, *Science* **311**, 1901(2006)
 - [6] P.B. Demorest, T. Pennucci, S.M. Ransom, M.S.E. Roberts, J.W.T. Hessels, *Nature* **467**, 1081(2010).
 - [7] J. Antoniadis , P.C.C. Freire , N. Wex , T.M. Tauris , R.S. Lynch, *Science* **340** , 448(2013).
 - [8] B.A. Li, L.W. Chen, C.M. Ko, *Phys Rep* **464**, 113(2008).
 - [9] R.N. Manchester, *Int. J. Mod. Phys. D* **24**, 1530018 (2015).
 - [10] V.M. Kaspi, M. Kramer, *arXiv* **1602.07738v1**(2016).
 - [11] D.H. Wen, W. Chen, *Chin. Phys. B* **20**, 029701(2011).
 - [12] Aaron Worley, Plamen G. Krastev, Bao-An Li, *Astrophys. J* **685**, 390(2008).
 - [13] G.B. Cook, S.L. Shapiro, S.A. Teukolsky, *Astrophys. J* **424**, 823(1994).
 - [14] J. Antoniadis, T.M. Tauris, F. Ozel, *arXiv* **1605**, 01665v1(2016).
 - [15] J.G. Martinez, K. Stovall, P.C.C. Freire, J.S. Deneva, *Astrophys J* **812**, 143(2015).
 - [16] P. Haensel, J.L. Zdunik, F. Douchin, *Astron. Astrophys* **385**, 301(2002).
 - [17] J.O. Goussard, P. Haensel, J.L. Zdunik, *Astron. Astrophys* **330**, 1005(1998).
 - [18] K. Strobil, C. Schaab, M.K. Weigel *Astron. Astrophys* **350**, 497(1999).
 - [19] K. Sumiyoshi, S. Yamada, H. Suzuki, W. Hillebrandt, *Astron. Astrophys* **334**, 159(1998).
 - [20] http://fast.bao.ac.cn/en/science_pulsar.html
 - [21] G. Baym, C.J. Pethick, P. Sutherland, *Astrophys. J* **170**, 299(1971).
 - [22] P. Haensel, B. Pichon, *Astron. Astrophys* **283**, 313(1994).
 - [23] J.W. Negele, D. Vautherin, *Nucl. Phys. A* **207**, 298(1973).
 - [24] G. Baym, H.A. Bethe, C.J. Pethick, *Nucl. Phys A* **175**, 225(1971).

- [25] C.J. Pethick, D.G. Ravenhall, C.P. Lorenz, Nucl. Phys. A **584**, 675(1995).
- [26] F. Douchin, P. Haensel, Astron. Astrophys **380**(1), 151(2001).
- [27] B. Friedman, V.R. Pandharipande, Nucl. Phys. A **361**, 502(1981).
- [28] E. Chabanat, P. Bonche, P. Haensel, J. Meyer, R. Schaeffer, Nucl. Phys. A **635**, 231(1998).
- [29] N. Chamel, Liv. Rev. Rel. **11**, 10(2008).
- [30] V.R. Pandharipande, Nucl. Phys. A **178**, 123(1971).
- [31] B.K. Harrison, K.S. Thorne, M. Wakano, J.A. Wheeler, eds., pp. 1-177, Chicago, University of Chicago Press(1965).
- [32] P.G. Krastev, F. Sammarruca, Phys. Rev. C **74**, 025808(2006).
- [33] S. Sammarruca, P. Liu, arXiv **0906**, 0320(2009).
- [34] A. Akmal, V.R. Pandharipande, D.G. Ravenhall, Phys. Rev. C **58**, 1804(1998).
- [35] J. Xu, L.W. Chen, B.A. Li, H.R. Ma, Astrophys. J **697**, 1549(2009).
- [36] C. Ducoin, J. Margueron, C. Providencia, I. Vidana, Phys. Rev. C **83**, 045810(2011).
- [37] F. Ozel, Nature **441**, 1115(2006)
- [38] K. Hebeler, J. M. Lattimer, C. J. Pethick, and A. Schwenk, Astrophys. J **773**,11(2013).
- [39] R. C. Tolman, Phys. Rev. **55**, 364 (1939).
- [40] J. R. Oppenheimer and G. M.Volkoff, Phys. Rev. **55**, 374(1939).
- [41] I. A. Morrison , T. W. Baumgarte ,S. L. Shapiro and V. R. Pandharipande, Astrophys. J **617** L135(2004).
- [42] J.R. Oppenheimer, R. Serber, Phys. Rev **54**, 540(1938).
- [43] S.L. Shapiro, S.A. Teukolsky, *Black holes, white dwarfs, and neutron stars: The physics of compact objects* (Wiley, New York City,1983).
- [44] N. K. Glendenning, *Compact Stars: Nuclear Physics, Particle Physics, and General Relativity* (Springer, New York, 2000).
- [45] S. Weinberg, *Gravitation and Cosmology: Principles and Applications of the General Theory of Relativity* (Wiley and Sons, New York, 1972).
- [46] L. Lindblom, Astrophys. J **398**, 569(1992).
- [47] F. Ozel , D. Psaltis, Phys. Rev. D **80**,103003(2009).
- [48] J.M. Lattimer, M. Prakash, Astrophys. J **550**, 426(2001).
- [49] A.G. Lyne, Science **303**, 1153(2004).
- [50] J.M. Lattimer, B.F. Schutz, Astrophys. J **629**, 979(2005).
- [51] F.J. Fattoyev, J. Piekarewicz, Phys. Rev. C **82**, 025810(2010)
- [52] J. Cottam , F. Paerels, M. Mendez, Nature **420** 51(2002).